





# Endolymphatic sac tumor mimicking an aneurysmal bone cyst

## *Tumor do saco endolinfático mimetizando um cisto ósseo aneurismático*

Carlos Dier<sup>1</sup>  Osorio Lopes Abath Neto<sup>2</sup>  Bruno Policeni<sup>3</sup>  Leonardo Furtado Freitas<sup>3</sup> 

<sup>1</sup>University of Iowa Hospitals and Clinics, Department of Neurology, Iowa City IA, United States.

<sup>2</sup>University of Iowa Hospitals and Clinics, Department of Pathology, Iowa City IA, United States.

<sup>3</sup>University of Iowa Hospitals and Clinics, Department of Radiology, Division of Neuroradiology, Iowa City IA, United States.

Address for correspondence Leonardo Furtado Freitas (email: drleonardofurtado@gmail.com).

Arq. Neuro-Psiquiatr. 2024;82(10):s00441789202.

A 61-year-old female patient presented with a large, right temporal mass causing hearing loss and vertigo. Imaging studies revealed multiple cysts, spiculated lesions, and heterogenous enhancement (► **Figures 1–3**). Soft-tissue components and epithelial cysts (► **Figure 4**) were recognized after surgery.

Endolymphatic sac tumors (ELSTs) are rare adenomatous neoplasms from the vestibular aqueduct's endolymphatic tissue.<sup>1</sup> These tumors are usually associated with Von Hippel Lindau disease.<sup>2</sup> Paragangliomas and hemangiomas should be included in the differential.<sup>3</sup> Endolymphatic sac tumors can mimic the imaging features of aneurysmal bone cysts.<sup>4</sup> Nevertheless, bone spicules and posterior petrous rim expansion on computed tomography and spontaneous hyperintense regions on magnetic resonance imaging suggest ELST.<sup>5</sup>

### Authors' Contributions

CD, OLAN, BP: conceptualization and validation; LFF: conceptualization, supervision, and writing – review & editing.

### Conflict of Interest

The authors have no conflict of interest to declare.

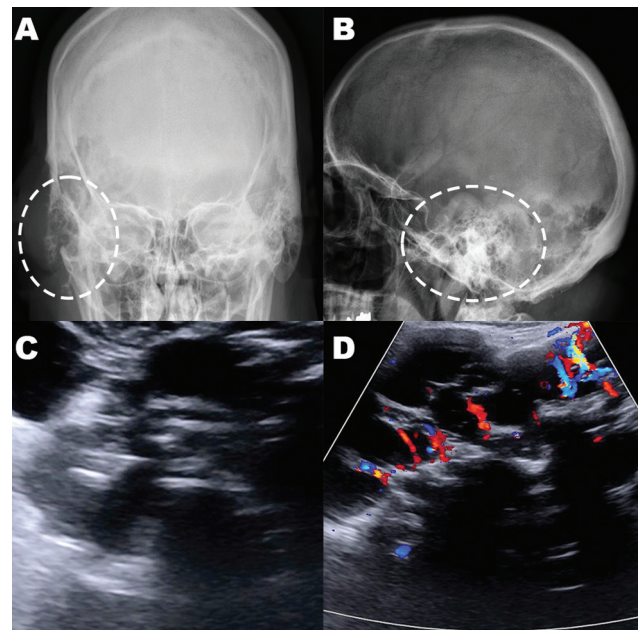


**Figure 1** Skull x-ray anteroposterior (A) and lateral (B) views showing a large predominantly cystic lesion in the right temporo-occipital region, with soft tissue component and extensive erosion of the mastoid trabeculae (dashed white circles). Superficial soft-tissue grayscale (C) and doppler (D) ultrasonography with anechoic content, multiple septations and mild vascularization.

received  
April 22, 2024  
accepted  
June 9, 2024

DOI <https://doi.org/10.1055/s-0044-1789202>.  
ISSN 0004-282X.

Editor-in-Chief: Ayrton Roberto Massaro.  
Associate Editor: Antonio José da Rocha.

© 2024. The Author(s).

This is an open access article published by Thieme under the terms of the Creative Commons Attribution 4.0 International License, permitting copying and reproduction so long as the original work is given appropriate credit (<https://creativecommons.org/licenses/by/4.0/>).  
Thieme Revinter Publicações Ltda., Rua do Matoso 170, Rio de Janeiro, RJ, CEP 20270-135, Brazil

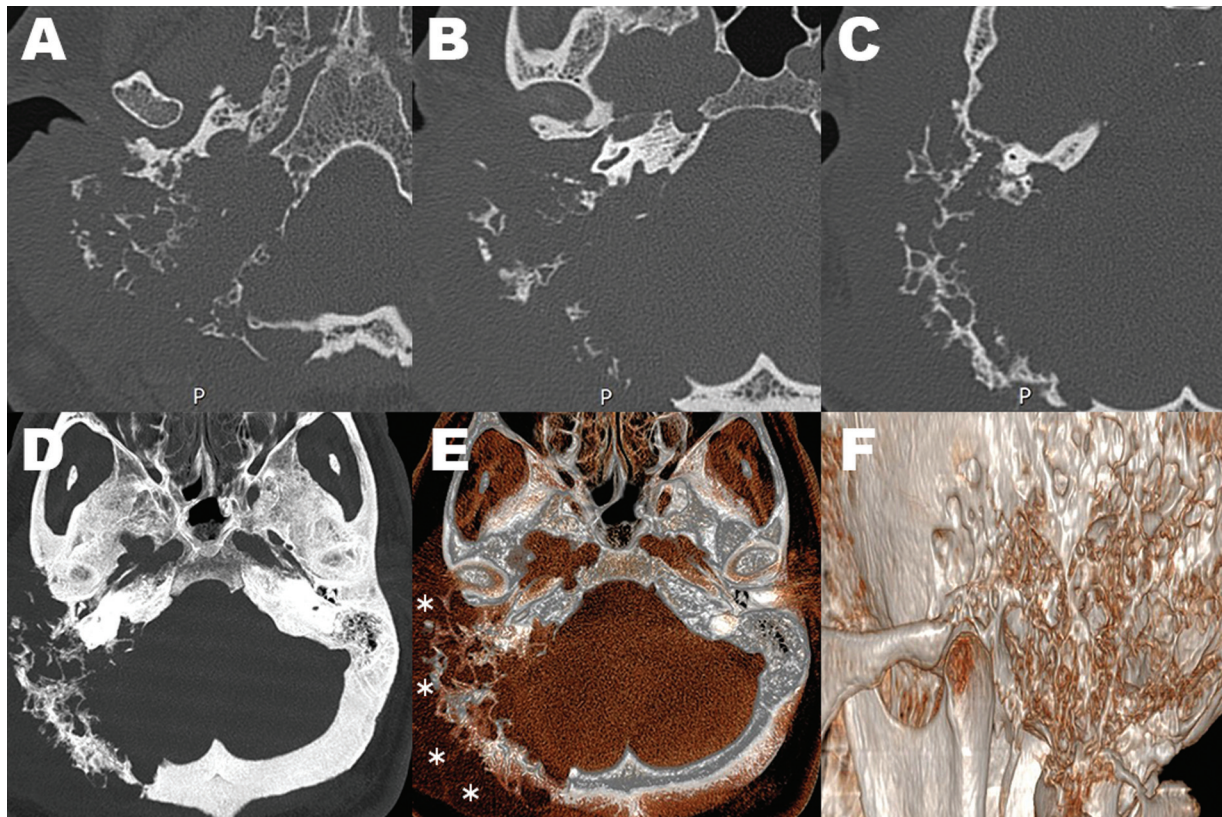


**Figure 2** High-resolution computed tomography images of the temporal bones (A-F). Giant destructive osseous lesion centered in the right mastoid and occipital bones. Multiple spiculated appearance and multicystic soft-tissue component (white asterisks) can be observed.

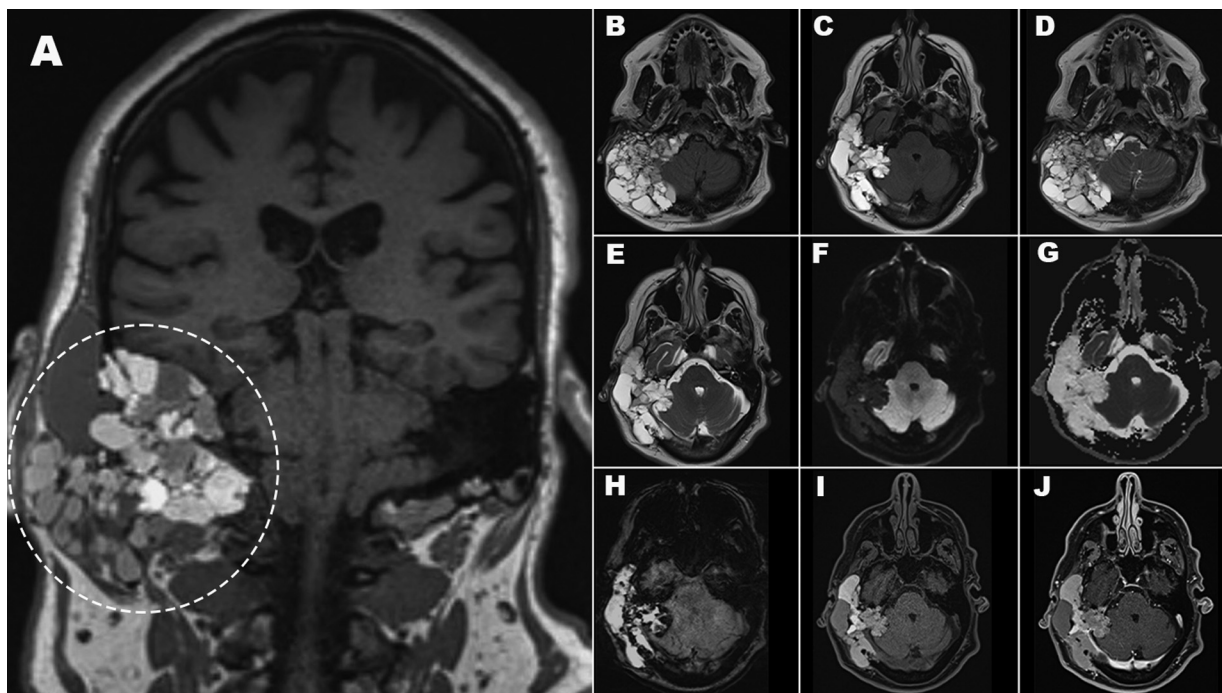


**Figure 3** Brain magnetic resonance imaging dedicated to posterior fossa evaluation. Coronal T1-weighted non-contrast (A), axial fluid-attenuated inversion recovery (B-C), axial T2-weighted (D-E), diffusion (F), apparent diffusion coefficient map (G), susceptibility-weighted imaging (H), and fat saturation T1 non-contrast (I), as well as fat saturation T1-weighted postgadolinium (J) images. Greater conspicuity of the heterogeneous cystic component, with variable signal due to hyper proteinaceous and hemorrhagic contents. There was facilitated diffusion and no significant enhancement.



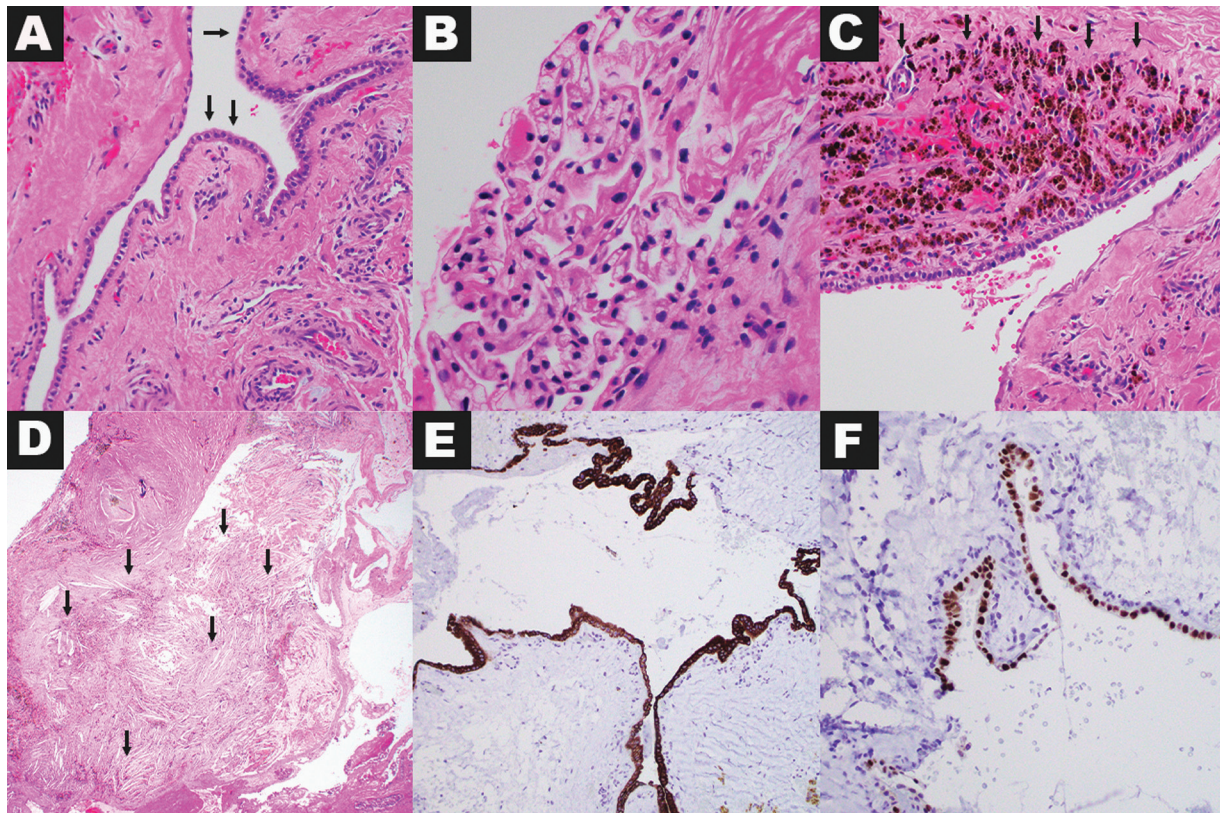


**Figure 4** Hematoxylin and eosin-stained slides (A and C, 200X; B, 400X, D, 40X) show multiple cysts lined by a single layer of epithelium (A, arrows), focally forming pseudopapillary arrangements (B). Cysts were associated with extensive hemorrhage and hemosiderin deposition, in many areas undermining the epithelium (C, arrows). Cholesterol clefts (D, arrows), morphologic indicators of longstanding tissue reaction, were present in cystic areas and within reactive soft tissue infiltrated by the tumor. Immunohistochemical stains show that the neoplastic cells are positive for pan-keratin (C, 100X) and PAX8 (D, 200X).

## References

- 1 Talukdar R, Epari S, Sahay A, et al. Endolymphatic sac tumor: single-institution series of seven cases with updated review of literature. *Eur Arch Otorhinolaryngol* 2022;279(05):2591–2598. Doi: 10.1007/s00405-021-07047-2
- 2 Tang JD, Grady AJ, Nickel CJ, et al. Systematic Review of Endolymphatic Sac Tumor Treatment and Outcomes. *Otolaryngol Head Neck Surg* 2023;168(03):282–290. Doi: 10.1177/01945998221108313
- 3 Wick CC, Manzoor NF, Semaan MT, Megerian CA. Endolymphatic sac tumors. *Otolaryngol Clin North Am* 2015;48(02):317–330. Doi: 10.1016/j.otc.2014.12.006
- 4 Alkonyi B, Günthner-Lengsfeld T, Rak K, Nowak J, Solymosi L, Hagen R. An endolymphatic sac tumor with imaging features of aneurysmal bone cysts: differential diagnostic considerations. *Childs Nerv Syst* 2014;30(09):1583–1588. Doi: 10.1007/s00381-014-2453-0
- 5 Le H, Zhang H, Tao W, et al. Clinicoradiologic characteristics of endolymphatic sac tumors. *Eur Arch Otorhinolaryngol* 2019;276(10):2705–2714. Doi: 10.1007/s00405-019-05511-8